Aggregation-Induced Emission in Tetraphenylthiophene-Derived Organic Molecules and Vinyl Polymer

ARTICLE *in* THE JOURNAL OF PHYSICAL CHEMISTRY B · AUGUST 2010

Impact Factor: 3.3 · DOI: 10.1021/jp1012297 · Source: PubMed

2 AUTHORS, INCLUDING:

Jin-Long Hong
National Sun Yat-sen University
83 PUBLICATIONS **794** CITATIONS

SEE PROFILE

THE JOURNAL OF PHYSICAL CHEMISTRY C

ARTICLE

pubs.acs.org/JPCC

Enhanced Aggregation Emission of Vinyl Polymer Containing Tetraphenylthiophene Pendant Group

Rong-Hong Chien, Chung-Tin Lai, and Jin-Long Hong*

Department of Materials and Optoelectronic Science, National Sun Yat-Sen University, Kaohsiung 80424, Taiwan, Republic of China

Supporting Information

ABSTRACT: In this study, poly[2-(4′-vinylphenyl)-3,4,5-triphenylthiophene] (PTP) with pendant tetraphenylthiophene (TP) groups was synthesized to study its aggregation-induced emission (AIE) property. The solution emission spectra of the PTP nanoaggregates contain discernible monomer and aggregate bands with their relative intensity dependent on the extent of aggregation. Increasing solution concentration or nonsolvent content resulted in the increase of the aggregate to monomer emission ratio. In addition, the aggregate to monomer emission ratio decreases when the PTP film was heated across the glass transition temperature (165 °C). Single-chain conformation of PTP was simulated to probe for the possible arrangements of the pendant TP fluorophores in the isolated (monomer) and the aggregate domains.

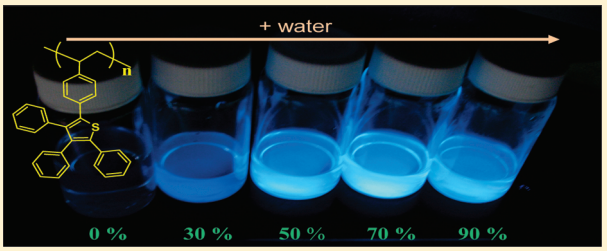

INTRODUCTION

Traditional organic fluorophores with multiple aromatic rings tend to aggregate with the favorable $\pi-\pi$ stacking interactions among their planar, disklike aromatic structures. Upon photo irradiation, the excited electrons in the concentrated solutions or in the solid state often decay nonradiatively and result in the aggregation-caused quench (ACQ) of emission.[1−7] Since fluorescent materials are normally used in the solid film state, development of efficient fluorophores with enhanced emission in the film state is of particular interest. One particular silole compound (1-methyl-1,2,3,4,5-pentaphenylsilole, Figure 1) with strong emission in the aggregated state was found by Tang's groups in 2001.[8,9] In contrast to the normal ACQ, silole compounds show the unusual "aggregation-induced emission" (AIE) behavior, in which the nonluminescence exhibited in the dilute solution can be converted to high luminescence if nanoaggregates of silole molecules were generated upon the introduction of the nonsolvent water.[8−14]

AIE-active fluorophores rendered hope for the fabrications of organic light-emitting diodes (OLEDs) with high performance since it confronts the ACQ problem encountered in the condensed solid application state. With this aspect, lots of organic fluorophores with the silole framework or with other chemical functions were developed and found to exhibit the AIE effect.[15−35] In the aggregated states of silole compounds, the restricted intramolecular rotation (IMR) of the phenyl rotors against the central silole stator reduces the nonradiative pathways and leads to the enhanced emission. With the structural blockage of the internal IMR, one regioisomer of diisopropyl-attached hexaphenylsilole compound was reported to emit strongly even in the pure solution state.[36] In addition to small-molecule fluorophores, several high molecular-weight polymers were also found to exhibit the AIE effect.[11,12,15,37−44] Among them, disubstituted polyaceylenes had been thoroughly studied and the vicinal phenyl rings in every monomer repeat unit hinder the conformational transformation process, which contributes to the restricted IMR process and the observed AIE phenomenon.[38]

With the chemical framework of one central thiophene stator connected by multiple peripheral aromatic rings, 2,3,4,5-tetraphenylthiophene (TP, Figure 1), TP-derived compound of TP-Qu, and vinyl polymer of PS-Qu had been previously prepared in our lab and were characterized to be AIE-active due to the restricted IMR.[45] Formations of aggregated nanoparticles of TP molecules in solvent/nonsolvent pair resulted in the emission enhancement. To contrast, solution photoluminescent (PL) emission spectra of TP-Qu are almost the same irrespective of the applied solvent/nonsolvent composition. The observed equivalent aggregate and solution emissions (EASE) are attributed to effective hindered rotation of the bulky diphenylquinoline ring of TP-Qu. The EASE phenomenon was also observed in the vinyl polymer of PS-Qu with TP-Qu pendant groups. Restricted IMR can be built with the use of hindered rotors, leading to fluorophores less affected by the surroundings.

In this study, we reported the new example of preparation of vinyl monomer vTP (Scheme 1) and its radical polymerization to generate vinyl polymer of PTP with TP pendant groups. Primary characterizations on the resultant PTP polymer reveal that it also exhibits the novel AIE properties. Unlike the precedent PS-Qu, the PTP polymer exhibits distinguishable monomer and aggregate emission bands. Thus, variations on monomer/aggregate

Received: November 6, 2010
Revised: February 8, 2011
Published: March 07, 2011

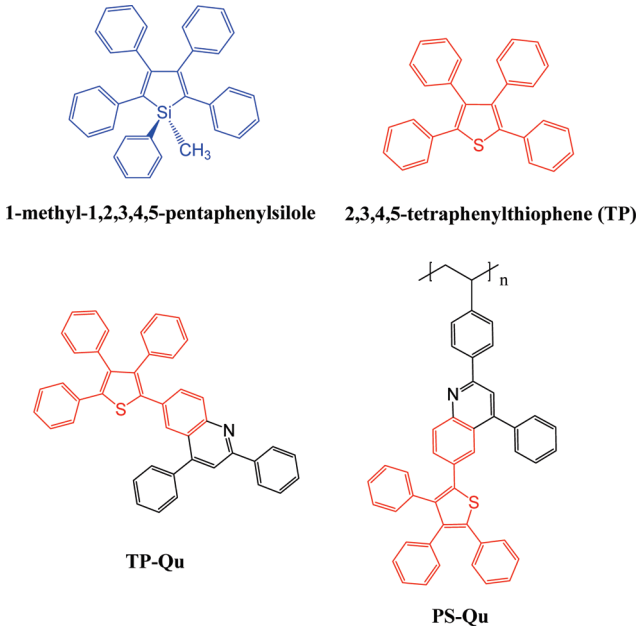

Figure 1. Chemical structures of 1-methyl-1,2,3,4,5-pentaphenylsilole, 2,3,4,5,-tetraphenylthiophene (TP), TP-derivative of TP-Qu, and vinyl polymer of PS-Qu.

emissions can be used to probe the relative extent of aggregation in different physical states (i.e., in the aggregated solution and in the solid or the viscous liquid states). The accompanied AIE effect in different physical aggregated states can be therefore studied and approached in this study.

EXPERIMENTAL SECTION

Materials. Aluminum chloride, acetyl chloride, sodium borohydride, *p*-toluenesulfonic acid monohydrate (TSA), and azobisisobutyronitrile (AIBN) were purchased from Aldrich Chemical Co. and used directly without further purification. Toluene and chloroform were refluxed over sodium under nitrogen for 2−3 days before distillation.

Syntheses of Small Molecules and Polymer. TP compound was prepared according to the reported procedures.[46−48] Monomer vTP and polymer PTP were prepared according to Scheme 1, and the detailed procedures are described below.

Preparation of 2-(4′-Acetylphenyl)-3,4,5-triphenylthiophene (TP-Ac). To a nitrogen-blanketed solution of TP (3 g, 7.7 mmol) in 20 mL of dry chloroform was added acetyl chloride (0.74 mL, 10 mmol) with stirring. Aluminum chloride (1.33 g, 10 mmol) was slowly added, and the whole mixture was then stirred for another day at room temperature. The solution product reaction mixture, after being cooled to room temperature, was poured into 50 g of ice. The organic phase was washed twice with 50 mL of water and dried over $MgSO_4$. After solvent evaporation, the crude product was purified by column chromatography (hexane/ethyl acetate = 9/1) to afford 2.5 g (yield: 76%) of TP-Ac. Mp: 156 °C. IR (KBr pellet, cm^{-1}, Figure S-5, Supporting Information) 3061, 2925, 1675, 1599, 1498, 1348, 1280, 845, 703. ^1H NMR (500 MHz, $CDCl_3$, Figure S-1, Supporting Information) δ 6.9−7.3 (m, 17H, aromatic Hc-Hg), 7.82 (d, 2H, aromatic Hb), 2.55 [s, 3H, —$CH_3C(=O)$]. MS *m*/*e*: calcd for $C_{30}H_{22}OS$, 430.14; found, 430.2 (M+). Anal. Calcd for $C_{30}H_{22}OS$: C, 83.69; H, 5.15; O, 3.72; S, 7.45. Found: C, 83.40; H, 5.21; O,3.51; S, 7.38.

Scheme 1. Preparation of vTP Monomer and the Subsequent Radical Polymerization To Yield Vinyl Polymer of PTP

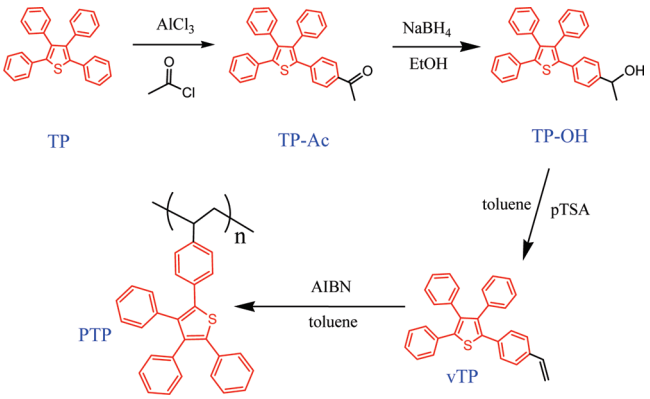

Preparation of 2-[4′-(1-Hydroxyethyl)phenyl]-3,4,5-triphenylthiophene (TP-OH). To a stirred solution of TP-Ac (1 g, 2.3 mmol) in 20 mL of ethanol was slowly added $NaBH_4$ (0.21 g, 4.8 mmol). The resulting mixture was then heated at 55 °C for one day. After cooling, 10 mL of 2% aq HCl solution was added to quench the unreacted $NaBH_4$. The organic layer was separated, washed with water (50 mL), dried over $MgSO_4$, and subjected to rotary distillation to yield an off-white solid. The crude product was then filtered and washed with water to give 0.62 g (yield: 63%) of TP−OH for further reaction. Mp: 216 °C. IR (KBr pellet, cm^{-1}) 3345, 3054, 2926, 1596, 1491, 1348, 1073, 1006, 835, 760, 707 (Figure S-5, Supporting Information). ^1H NMR (500 MHz, $CDCl_3$, Figure S-2, Supporting Information) δ 6.9−7.3 (m, 19H, aromatic Hd-Hi), 5.3 (s, 1H, -O*H*), 4.8(dd, 1H, C*H*), 1.4 (s, 3H, $-CH_3$). MS *m*/*e*: calcd for $C_{30}H_{24}OS$, 432.15; found, 432.5 (M+). Anal. Calcd for $C_{30}H_{24}OS$: C, 83.30; H, 5.59; O, 3.70; S, 7.41. Found: C, 83.20; H, 5.51; O,3.71; S, 7.35.

Preparation of 2-(4′-Vinylphenyl)-3,4,5-triphenylthiophene (vTP). A solution of TP-OH (0.4 g, 0.93 mmol) and toluene sulfonic acid (0.02 g; 0.11 mmol) in 80 mL of dry toluene were heated to reflux in a Dean−Stark apparatus. Continuous removal of the distillate was accompanied by occasional additions of dry toluene. Reaction was monitored by TLC analysis and was completed after 24 h. After cooling, the resulting solution was concentrated to ca. half of the volume. The resulting mixture was then mixed with 30 mL of chloroform, washed twice with 30 mL of 1 N aq Na_2CO_3 solution and twice with 40 mL of water, and dried over Na_2SO_4. After removal of solvent, the crude product was then purified by column chromatography ($CHCl_3$) to obtain 0.26 g (yield: 68%) of vTP monomer as a white powder. Mp: 131 °C. IR (KBr pellet, cm^{-1}) 3048, 2926, 1625, 1604, 1500, 1432, 901, 1006, 841, 775, 701 (Figure S-6, Supporting Information). ^1H NMR (500 MHz, $CDCl_3$, Figure S-3, Supporting Information) δ 6.5−7.3 (m, 19H, aromatic Hd-Hi), 6.5−6.7 (q, 1H, —C*H*=CH_2), 5.7 (d, 1H, —CH=C*H*), 5.2 (d, 1H, —CH=C*H*). MS *m*/*e*: calcd for $C_{30}H_{22}OS$, 414.56; found, 414.7 (M+). Anal. Calcd for $C_{30}H_{22}OS$: C, 86.92; H, 5.35; S, 7.73. Found: C, 86.40; H, 5.29; S, 7.55.

Preparation of Poly[2-(4′-vinylphenyl)-3,4,5-triphenylthiophene] (PTP). A solution of vTP (0.2 g, 0.48 mmol) and AIBN (3.3 mg; 0.005 mmol) in 3 mL of toluene was heated at 80 °C for 72 h.

The reaction mixture was then poured into large amounts of water to precipitate the pale yellow product (0.11 g, yield 55%). GPC (eluent: THF, Figure S-8, Supporting Information): M_n = 9600, M_w = 16 400, and PDI = 1.71. T_g: 165 °C (Figure S-7, Supporting Information). IR (KBr pellet, cm^{-1}) 3056, 3023, 2926, 1595, 1568, 1505, 1442, 1402, 1263, 1097, 1026, 802 (Figure S-6, Supporting Information). ^{1}H NMR (500 MHz, $CDCl_3$, Figure S-4, Supporting Information) δ 6.9−7.3 (m, 19H, aromatic Hs), 1.25 (3H, backbone Hs′).

Instrumentation and Sample Preparation. ^{1}H NMR spectra were recorded with a Varian VXR-500 MHz FT-NMR spectrometer. Tetramethylsilane was used as internal standard. A VG Quattro GC/MS/MS/DS instrument was used to determine the molar mass of the organic molecules. Molecular weight and molecular weight distribution of PTP polymer were determined from GPC using a Waters 510 HPLC model equipped with a 410 differential refractometer, a UV detector, and three Ultrastyragel columns (100, 500, and 1000 Å) connected in series. Polymer solution was eluted by THF with a flow rate of 0.6 mL/min. The molecular weight calibration curve was obtained from polystyrene standards. The glass transition temperatures (T_g's) of PTP polymer were obtained from a TA Q-20 DSC calorimeter. The scan rate was 20 °C/min, and the sample (~10 mg) was primarily held at 300 °C for 3 min and then cooled rapidly to −50 °C before rescan to obtain the thermogram. FT-IR spectra were obtained from a Nicolet IR-200 spectrometer. A solution of organic compound or polymer in THF was dropped on a KBr pellet and dried at 100 °C under vacuum to prepare a solid film for FT-IR analysis.

PL was obtained from a LabGuide X350 fluorescence spectrophotometer using a 450W Xe lamp as the continuous light source. UV−vis absorption spectra were recorded with an Ocean Optics DT 1000 CE 376 spectrophotometer. Small quartz cell with dimensions 0.2 × 1.0 × 4.5 cm^3 was used to accommodate the solution sample. Stock solutions (10^{-4} M) of organic and polymeric fluorophores in THF were primarily prepared. An aliquot of the stock solution was then transferred to a 10 mL volumetric flask, into which an appropriate volume of THF and water was added dropwise under vigorous stirring to furnish 10^{-5} M solutions with different water contents (0−90 vol %). A solid specimen was prepared by drop-casting sample solution on a quartz plate. UV−vis and PL emission spectra were immediately taken once the solutions were prepared. Particle sizes were measured by a dynamic light scattering (DLS) instrument on a Brookhaven 90 plus spectrometer at room temperature. An argon ion laser operating at 658 nm was used as light source. The conformation of PTP was formulated from the Materials Studio (MS) commercial software of Accelrys Inc.[38,45]

RESULTS AND DISCUSSION

Synthesis. The vinyl polymer PTP with the fluorophoric pendant TP group was prepared from the radical polymerization of monomer vTP according to Scheme 1. Monomer vTP was synthesized from the organic compound TP[46−48] through a three-step reaction procedure starting from monoacetylation of TP to obtain TP-Ac, hydrogenation of TP-Ac to generate TP-OH, and the following dehydration of TP-OH. Polymer PTP was thereby generated from radical polymerization of monomer vTP at 80 °C using AIBN as initiator. The organic compounds of TP-Ac, TP-OH, and vTP were purified by column chromatography and instrumentally identified (spectroscopy data of ^{1}H NMR in Figures S-1 to S-4, and FTIR in Figure S-5 to S-6, Supporting Information). The resulting polymer PTP has M_n = 9600, M_w = 16 400, and PDI = 1.71 according to GPC analysis (Figure S-7, Supporting Information) and is amorphous in nature according to the detected T_g with midpoint at 165 °C (from the DSC thermogram, Figure S-8, Supporting Information). The bulky TP pendants of PTP stiffen the polymer main chain and lead to the observed high T_g. The resultant vinyl polymer of PTP is readily soluble in common organic solvents such as chloroform, methylene chloride, THF, and toluene.

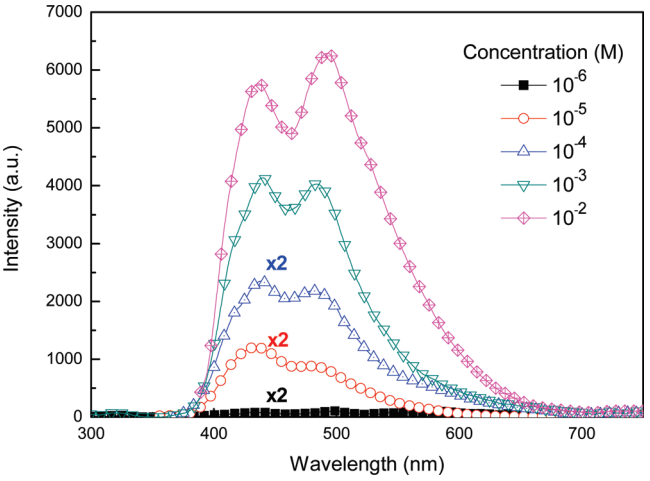

Figure 2. Photoluminescent spectra of PTP in THF of various concentrations. (excited at 330 nm).

AIE Effect. Effect of concentration was emphasized by the unnormalized PL emission spectra in Figure 2, which exhibited the continuous accession of the emission intensity with increasing concentration. Whereas solution thickening often quenches light fluorophore's emission, PTP solutions become more emissive with higher concentration. This peculiar phenomenon of concentration-enhanced emission is possibly due to the AIE effect, as we will discuss later. Here, solution (10^{-6} M) with very low fluorophore content is essentially weak in emission, but from dilute (1×10^{-5} M) to concentrated (1×10^{-2} M) solutions, two overlapping emission bands started to emerge and to have enhanced emission magnitudes with increasing concentration. With increasing concentration, the long-wavelength emission became more intense than the short-wavelength one. Also, the emission maximum of the short-wavelength emission remained at the same position of 437 nm, which is contrary to the observed red-shift of the long-wavelength emission. The short- and long-wavelength emissions are supposed to be due to the monomer and the aggregation emissions, respectively.

The AIE effect can also be characterized by examining the emission behavior of PTP in solvent mixtures with different fractions of THF and water. Since water is nonsolvent for PTP, the hydrophobic polymer chains of PTP are considered to form aggregates in the THF/water mixtures. Mixtures of PTP in THF/water were vigorously stirred to ensure uniform dispersion of the polymer aggregates before emission measurements. All the resultant mixture solutions (10^{-5} M, relative to repeat unit) are macroscopically homogeneous but visually opaque with no precipitate even at a high water fraction of 90 vol % water, indicating formation of nanoparticles upon water addition. All the opaque suspensions are quite stable without visible precipitation for a long period (>2 months). Formations of nanoparticles

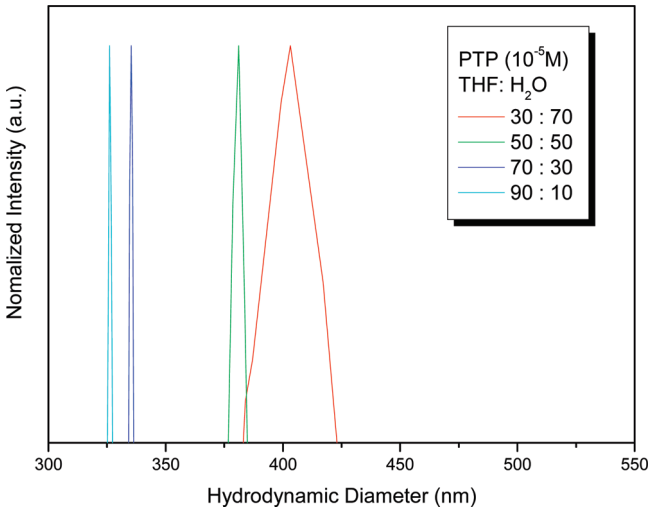

Figure 3. Hydrodynamic diameter of PTP (10^{-5} M) in THF/water mixture solvent with different ratios (v/v %).

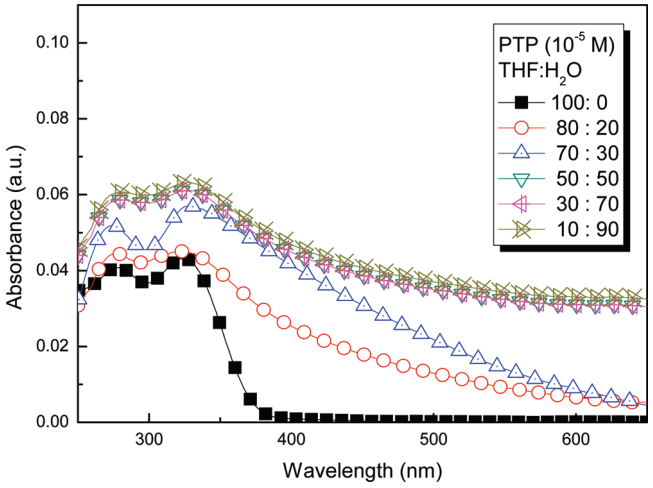

Figure 4. UV−vis absorption spectra of PTP (10^{-5} M) in THF/water mixtures with different ratios (v/v %).

can be confirmed by the particle size measurements from DLS (Figure 3). No signal is recorded from the polymer solution in pure THF, indicating that polymer PTP is genuinely dissolved in the good solvent of THF. On the contrary, polymer aggregates with average diameters of 325−400 nm are detected in the THF/water mixtures with various water contents. The hydrodynamic diameters detected here are even larger than the extended length of a single polymer chain, indicating that aggregations of polymer chains actually occurred in the dilute solution state (for 10^{-5} M solution, the content of PTP is less than 0.1 wt %). The results in Figure 3 also suggest that the suspended nanoparticles tended to shrink in size with increasing water content in the mixtures, which is reasonable, considering that shrinkage of the hydrophobic polymer aggregates reduced the unfavorable contacts with the majority water matrix. The volume shrinkage directly leads to more effective restrictions on the IMR of the fluorophoric TP pendants, a point that will be verified later.

The UV−vis absorption and the PL emission spectra of PTP in THF/water solvent mixtures were conducted to identify the AIE effect. The short- and long-wavelength bands in the solution

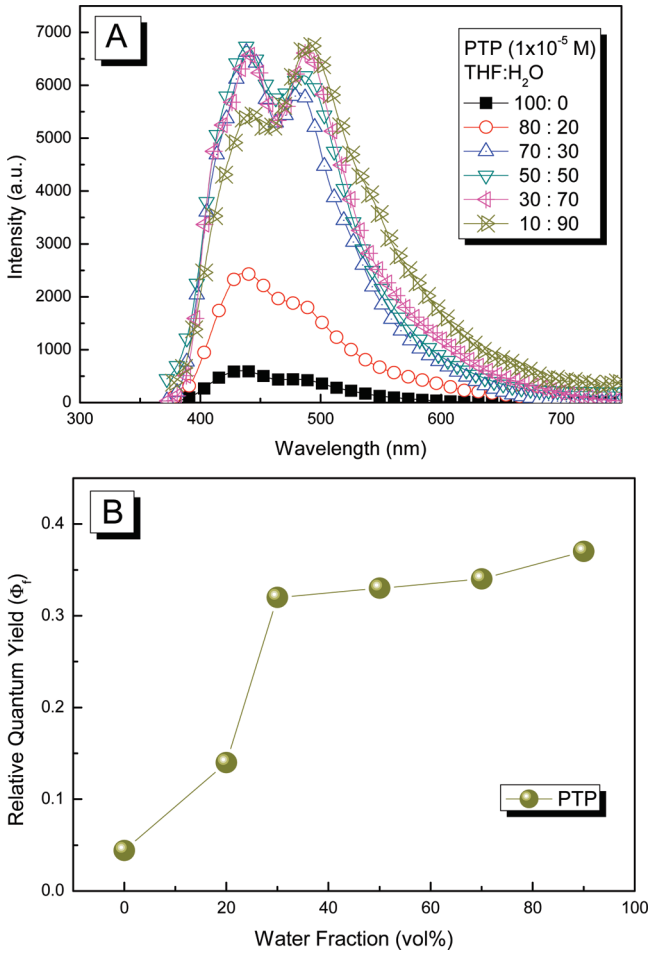

Figure 5. (A) Photoluminescent emission spectra of PTP (10^{-5} M) in THF/water mixtures with different ratios (v/v %; excited at 330 nm) and (B) the measured quantum yields from the corresponding solution mixtures.

UV−vis absorption spectra (Figure 4) of PTP in THF/water mixtures are supposed to be due to absorptions from the more isolated (monomer) species and from species in the aggregated regions, respectively. With increasing content of water from 0 to 80 vol %, the monomer absorption peak remained at the same position of 281 nm, but the maxima of the aggregate absorption shifted from 323 to 330 nm. A red shift of the aggregation band with the water addition had also been found for other AIE-active materials such as silole, butadiene, and dibenzofulvene series.[8,9,18,25,26] Except for a solution of PTP in pure THF, all other solutions exhibited a level-off long-wavelength (>400 nm) tail, which is attributed to the Mie scattering[49,50] from the nanoaggregates formed in the solution mixtures, a phenomenon also observed in other AIE-active materials.[10,14,17,18,20,25] The PL emissions excited at 330 nm (mostly from aggregated emission) have larger emission intensities than the emissions excited at 281 nm (basically, from monomer emission), which alternatively manifests the more decisive role of aggregates on emission enhancement as compared to the monomer emission.

Upon excitation at 330 nm, dilute solution (10^{-5} M) of PTP in pure THF emitted weakly (Figure 5A), and with the increasing water additions, the corresponding solution mixtures exhibited a large increase in the emission intensity. For the 90 vol % water solution, more than 8-fold emission enhancement was observed

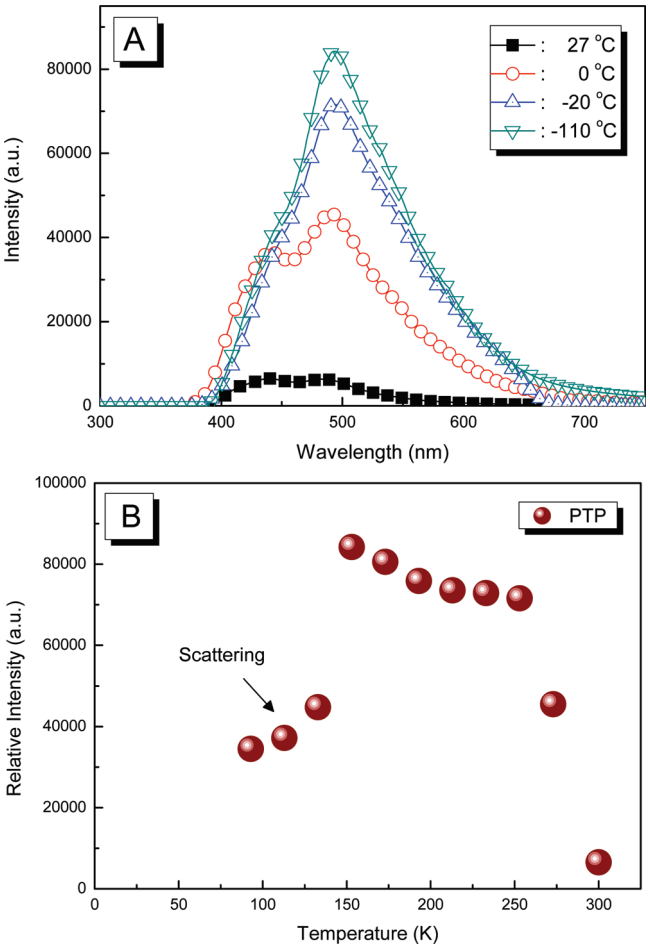

Figure 6. (A) Photoluminescent emission spectra of solution (10^{-5} M) of PTP in DMF at reduced temperatures (excited at 330 nm) and (B) the integrated area of the PL emission spectra in part A versus temperatures.

compared to PTP in pure THF. As described above, the two emissions in the short- and long-wavelength regions are due to the monomer and the aggregate emissions, respectively. The aggregate emissions gradually shifted to longer wavelengths with increasing water content. In accordance with Figure 2, the aggregation emission became more intense than the monomer emission when the extent of aggregation was increased upon water addition.

The AIE effect of PTP polymer can be further identified from the fluorescent quantum yield (Φ_f). The resultant Φ_f's of PTP in THF/water mixtures were summarized in Figure 5B. Solution of PTP in pure THF has a low Φ_f of 0.0442. Values of Φ_f changed abruptly when water content reached 30 vol % and then increased inconspicuously with further increase of water content in the solvent mixtures. The results are coherent with fluorescence spectra in Figure 5A. Solution of PTP in 10:90 THF/H_2O has a high Φ_f value of 0.37, which is ~8.4 times that from PTP in pure THF. The value of Φ_f measured from the solid PTP is 0.55, indicating an even higher extent of aggregation in the solid than in the solution aggregate states.

Solution PL Emission at Reduced Temperature. The solution PL emission spectra of PTP at reduced temperature were then studied with the purpose of evaluating the influence of IMR and aggregation on the PL emission. Temperature lowering results in the reduction of the revolving motions of the aromatic fluorophore and their interactions with the surrounding molecules (mostly the solvent molecules in dilute solution) and, thus, hampers the nonradiative process and enhances the solution emission. As resembling silole compounds,[8,9] the TP pendant of the PTP polymer has a chemical structure with the multiple peripheral phenyl rotors linked by the same stator; therefore, the restricted IMR responsible for the AIE of silole compounds should be analogously operative for polymer PTP, too. In this study, PTP possesses distinguishable aggregate and monomer emission bands; therefore, degree of aggregation in relationship to temperature can be evaluated from the low-temperature PL spectra. With reduced temperature, coil size of polymer in dilute solution will shrink, leading to the reduced intrachain distances and the enhanced intrachain aggregation. Since the PL emission of the AIE-active PTP relates to extent of aggregation, the intensity ratio between the aggregate and the monomer emissions at reduced temperature can be therefore used to probe for the extent of intrachain aggregation in dilute solution.

The enhanced emissions at lower temperatures were indeed verified by cooling the dilute solution (10^{-5} M) of PTP in DMF. By cooling dilute solution of PTP from room temperature to −110 °C, the long-wavelength aggregate emission (Figure 6A) largely increased in intensity, contrary to the relatively small enhancements on the monomer emission. The large enhancement of the aggregate emission occurred in the initial cooling stage from room temperature to −20 °C, which caused the great jump in the integrated emission intensity shown in Figure 6B. Continuous cooling from −20 to −120 °C has less effect on the intensity than the initial cooling step. Further cooling to temperatures (−120 to −180 °C) well below the melting point (−61 °C) of DMF media resulted in the freezing of DMF solvent and the accompanied scattering of the incident light, which caused reduction of the integrated intensity in the referred regions.

Solid PL Emission at High Temperature. Aggregation of polymer chain and the corresponding molecular motions should be greatly altered in passing over the glass transition. The solid PTP was then heated to temperatures above T_g to probe the extent of aggregation by the PL emissions since it correlates with the corresponding aggregation of the fluorophores in different physical states. The selected PL emission spectra in Figure 7A illustrate the gradual transformations of the emission patterns when heated from 140 to 200 °C (>165 °C, T_g of PTP). When heated below 140 °C, the resolved PL spectrum contains mostly the aggregate emission band, indicating that the extent of aggregation in the solid sample is higher than that in the solution mixture (compare with Figure 5). When further heated to above 170 °C, the monomer emission increased its contribution at the expense of the long-wavelength aggregation emission. The reduction of the aggregate emission was accompanied by the blue shift of the emission maxima, which is consistent with the trend observed in the solution PL spectra in Figure 5. The integrated emission intensities across the glass transition temperature were summarized in Figure 7B, which emphasizes the emission reductions when heated at temperatures across the glass transition. By heating PTP at temperatures above T_g, the corresponding thermal agitation promotes the molecular motions of the polymer segments and largely reduces the emission originated from the AIE effect. More planar structures originally existing in the solid aggregates will be dissociated and result in the less conjugated structures and the corresponding blue shift.

Samples at 200 °C were then quenched in liquid nitrogen to obtain a solid film to compare with the pristine solvent-cast

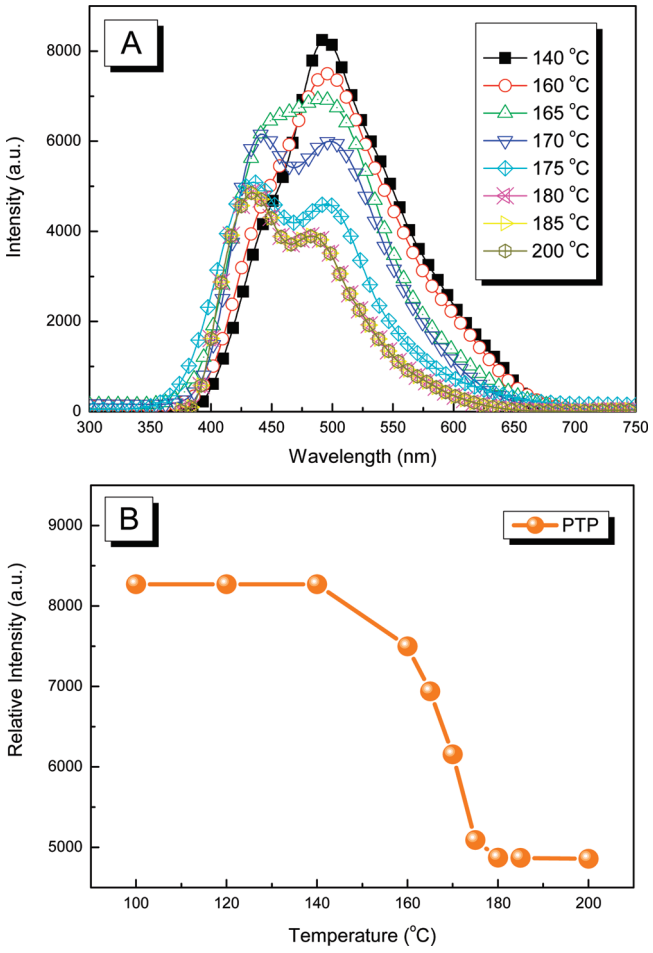

Figure 7. (A) Photoluminescent emission spectra of solid PTP at elevated temperatures (excited at 330 nm) and (B) the integrated area of the PL emission spectra in part A versus temperatures.

Table 1. Data Calculated from the Fluorescent Decay Curves

wavelength (nm)	A_1 (%)	A_2 (%)	$\tau_1{}^a$ (ns)	$\tau_2{}^a$ (ns)	$\langle\tau\rangle^b$ (ns)
Solvent-Cast PTP Sample					
440	75	25	0.75	4.69	1.74
490	30	70	0.30	9.61	6.82
Quenched PTP Sample					
440	82	18	0.80	4.23	1.42
490	44	56	0.19	7.32	4.18

[a] Determined from the fitting function of $y = A_1e^{-t/\tau 1} + A_2e^{-t/\tau 2}$ from the fluorescence decay curves in Figure S-9. [b] Determined from $\langle\tau\rangle = (A_1\tau_1 + A_2\tau_2)/(A_1 + A_2)$.

sample for the fluorescent decay behavior. The time-resolved fluorescence spectra (Figure S-9, Supporting Information) of the solvent-cast and the quenched samples were monitored at two wavelengths, 400 and 490 nm. The resolved data form the corresponding decay curves were quantitatively fitted with the double-exponential function

$$y = A_1e^{-t/\tau_1} + A_2e^{-t/\tau_2}$$

since it yields better results than the single-exponential one. The monomeric and the aggregated decaying with the representative fractions of A_1 and A_2 can be characterized by the respective lifetimes of τ_1 and τ_2. As summarized in Table 1, the long-lived excited species decay with longer lifetime of τ_2 as compared to the short-lived species with shorter lifetimes of τ_1. Values in Table 1 suggest that the lifetime from the 440-nm light results in more fractions of fast-decay pathways, in contrast to the more slow-decay processes resolved from the 490-nm decaying curves. The fast-decay pathways are therefore due to the excited species in more isolated (monomer) units while the slow-decay pathways are from the paired species in the aggregated regions. Heating at 200 °C tends to generate more monomeric species, which contributes to the increasing values of A_1 in the quenched samples as compared to the solvent-cast ones. Average lifetime $\langle\tau\rangle$ can be also formulated from

$$\langle\tau\rangle = (A_1\tau_1 + A_2\tau_2)/(A_1 + A_2)$$

and the results suggest a longer average lifetime for the solvent-cast samples when compared to the quenched samples.

Chain Conformation from Computer Simulation. Since the fluorophoric TP pendants of the PTP polymer are separated by 3 carbon atoms, PTP may follow the "n = 3" rule to have the intramolecular excimer emission like other molecules [such as 1,3-diphenylpropane, polystyrene (PSt)[51,52] and substituted polyacetylenes (PAcs)].[38] Nevertheless, only monomer and aggregate emissions were observed for PTP in this study. This may be due to certain structural differences between PTP and other molecules following the n = 3 rule. First, unlike the small phenyl pendants of PSt, the bulky, vicinal TP pendants in PTP are difficult to pack in a near face-to-face parallel geometry between the vicinal 1,3-pendant pair, which is a prerequisite for the excimer formation. On the other hand, the flexible aliphatic main chain (—CH_2—CH—) of PTP is difficult to keep in a rigid conformation as compared to the pendant fluorophores attached in the rigid vinylene main chain (—C═C—) of PAcs. To qualitatively understand the possible arrangement of the vicinal TP pendants, theoretical simulation on the chain conformation of PTP was performed with the use of Material Studio software package. Vinyl polymer of PTP with 23 monomer units (corresponding to a molecular weight of 9500 g/mol, close to the detected M_n of 9600) was constructed, and its energy was minimized using the Smart Minimizer incorporated in the Discover Molecular Simulation program. Figure 8 depicts the chain structure after conformation optimization and energy minimization. Some unpaired TP pendant groups (marked by red arrow) stood alone and are the possible sources for the observed monomer emission. Also, there are some domains (circled area) containing sequential TP fluorophores packed intimately but in nonparallel manners. These intimately packed domains are the aggregated regions responsible for the observed aggregate emission.

Emission response of PTP in dilute solution can be explained by the variations of polymer chain conformation with the addition of water nonsolvent. The solvating power of THF toward the hydrophobic PTP is reduced with the addition of water nonsolvent. The polymer chains in dilute solution will then change the conformation from extended coil to shrunk aggregated nanoparticles in order to reduce the unfavorable contact surface with water. The shrunk aggregated nanoparticles have reduced sizes (as evidenced from the DLS results in Figure 3) and compact structure with closer interchain distances compared

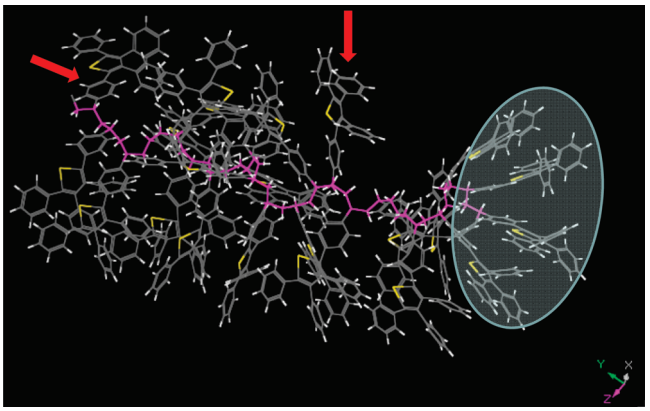

Figure 8. Simulated chain conformation of PTP segment with 23 monomer units (isolated monomer unit is pointed to by red arrow, and the circled area refers to aggregated units).

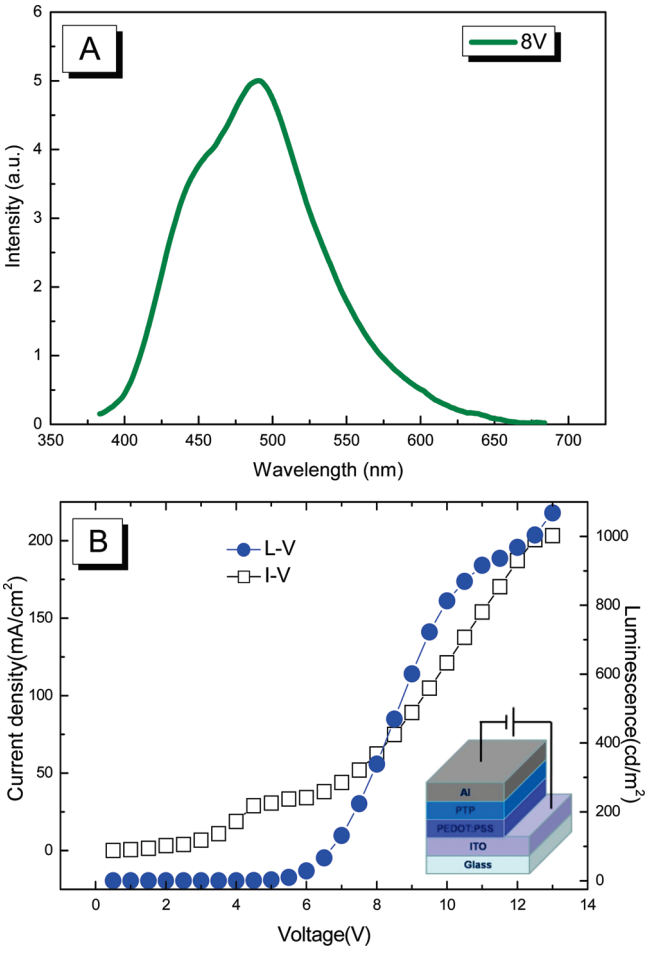

Figure 9. (A) Electroluminescent spectrum of PTP at 8 V. Device structure was ITO/PEDOT:PSS (100 nm)/PTP (150 nm)/Al (120 nm). (B) Current density and luminance vs voltage characteristics of polymer PTP.

to the extended chains. Certain isolated fluorophores in the extended polymer chains (as in the simulated single-chain conformation in Figure 8) will then contact other fluorophores in other polymer chains, which resulted in the decrease of monomer emission (therefore, the increase of aggregate emission). The intimate contacts rigidify the polymer chain and enhance the $\pi-\pi$ stacking interactions of the phenyl rings and the red-shift of the PL emission spectra. The congestion caused by the neighboring bulky TP pendants makes the polymer chain difficult to undergo conformational transformation during the aggregate formation. In other words, the nonradiative decay process will be hindered due to the restricted molecular motions, and this caused the enhanced emissions in the aggregated suspension.

Device Performance. Preliminary EL devices were fabricated with a configuration of ITO/PEDOT:PSS (100 nm)/PTP (80 nm)/Al (120 nm), and encapsulation was performed under a nitrogen atmosphere. EL spectrum of PTP copolymers is shown in Figure 9A). The spectrum consists of the main aggregate emission band centered at ~490 nm and the small shoulder-like monomer emission at ~440 nm. The spectrum is essentially similar to the solid state PL emissions. Preliminary device performances are encouraging. The current density (I, mA/cm^2)−voltage (V) and the luminance (L, cd/m^2)−bias voltage (V) for the devices from PTP were shown in Figure 9B. The device shows a low operating voltage onset at ~5.0 V, and in addition, a high luminance of 1000 cd/m^2 was reached at a bias voltage of 13 V. The resultant properties suggest that PTP can serve well as the emitting layer in the LED devices.

CONCLUSIONS

Vinyl polymer of PTP prepared from radical polymerization of TP monomer shows novel AIE properties. The emission intensity and the aggregate/monomer emission ratio in the solutions can be enhanced by varying the experimental variables such as increasing concentration, introducing nonsolvent water, and cooling the solutions to low temperatures. For PTP film, the aggregate/monomer emission ratio can be alternatively reduced by heating to temperature above T_g (165 °C). Results from the time-resolved fluorescence spectra reveal the longer lifetime of aggregate emission as compared to monomer emission. Simulated single-chain conformation suggests that the isolated (monomer) species and the intimately packed (aggregated) TP pendants are responsible for the observed monomer and aggregate emissions, respectively.

ASSOCIATED CONTENT

Supporting Information. Sample characterizations (^{1}H NMR, FTIR, DSC, and GPC) and results from the time-resolved fluorescence decay curves of solvent-cast and quenched samples of PTP monitored at the respective wavelengths of 440 and 490 nm. This material is available free of charge via the Internet at http://pubs.acs.org.

AUTHOR INFORMATION

Corresponding Author

*E-mail: jlhong@mail.nsysu.edu.tw. Phone: +886-7-5252000 ext 4065.

ACKNOWLEDGMENT

We appreciate the financial support from the National Science Council, Taiwan, Republic of China, under Contract NSC 98-2221-E-110-005-MY2.

REFERENCES

(1) Birks, J. B. *Photophysics of Aromatic Molecules*; Wiley: London, 1970.

(2) Thomas, S. W., III; Joly, G. D.; Swager, T. M. *Chem. Rev.* **2007**, *107*, 1339–1386.

(3) Belletête, M.; Bouchard, J.; Leclerc, M.; Durocher, G. *Macromolecules* **2005**, *38*, 880–887.

(4) Chen, C. T. *Chem. Mater.* **2004**, *16*, 4389–4400.

(5) Grell, M.; Bradley, D. D. C.; Ungar, G; Hill, J.; Whitehead, K. S. *Macromolecules* **1999**, *32*, 5810–5817.

(6) Jakubiak, R.; Collison, C. J.; Wan, W. C.; Rothberg, L. *J. Phys. Chem. A* **1999**, *103*, 2394–2398.

(7) Lemmer, U.; Heun, S.; Mahrt, R. F.; Scherf, U.; Hopmeier, M.; Siegner, U.; Gobel, E. O.; Müllen, K.; Bassler, H. *Chem. Phys. Lett.* **1995**, *240*, 373–378.

(8) Xie, J. Z.; Lam, J. W. Y.; Cheng, L.; Chen, H.; Qiu, C.; Kwok, H. S.; Zhan, X.; Liu, Y.; Zhu, D.; Tang, B. Z. *Chem. Commun.* **2001**, 1740–1741.

(9) Tang, B. Z.; Zhan, X.; Yu, G.; Lee, P. P. S.; Liu, Y.; Zhu, D. *J. Mater. Chem.* **2001**, *11*, 2974–2978.

(10) Chen, J.; Xie, Z.; Lam, J. W. Y.; Law, C. C. W.; Tang, B. Z. *Macromolecules* **2003**, *36*, 1108–1117.

(11) Ren, Y.; Dong, Y.; Lam, J. W. Y.; Tang, B. Z.; Wong, K. S. *Chem. Phys. Lett.* **2005**, *402*, 468–473.

(12) Ren, Y.; Lam, J. W. Y.; Dong, Y.; Tang, B. Z.; Wang, K. S. *J. Phys. Chem. B* **2005**, *109*, 1135–1140.

(13) Wang, M.; Zhang, D.; Zhang, G.; Zhu, D. *Chem. Phys. Lett.* **2009**, *475*, 64–67.

(14) Chen, J.; Law, C. C. W.; Lam, J. W. Y.; Dong, Y.; Lo, S. M. F.; Williams, I. D.; Zhu, D.; Tang, B. Z. *Chem. Mater.* **2003**, *15*, 1535–1546.

(15) Hong, Y.; Lama, J. W. Y.; Tang, B. Z. *Chem. Commun.* **2009**, 4332–4353.

(16) Bhongale, C. J.; Hsu, C.-S. *Angew. Chem., Int. Ed.* **2006**, *45*, 1404–1408.

(17) Tong, H.; Hong, Y.; Dong, Y.; Häussler, M.; Lam, J. W. Y.; Guo, Z.; Li, Z.; Guo, Z.; Tang, B. Z. *Chem. Commun.* **2006**, 3705–3707.

(18) Tong, H.; Dong, Y.; Hong, Y.; Häussler, M.; Lam, J. W. Y.; Sung, H. H.-Y.; Yu, X.; Sun, J.; Williams, I. D.; Kwok, H. S.; Tang, B. Z. *J. Phys. Chem. C* **2007**, *111*, 2287–2294.

(19) Dong, S.; Li, Z.; Qin, J. *J. Phys. Chem. B* **2009**, *113*, 434–441.

(20) An, B. K.; Kwon, S. K.; Jung, S. D.; Park, S. Y. *J. Am. Chem. Soc.* **2002**, *124*, 14410–14415.

(21) Wang, Z.; Shao, H.; Ye, J.; Tang, L.; Lu, P. *J. Phys. Chem. B* **2005**, *109*, 19627–19633.

(22) Tong, H.; Hong, Y.; Dong, Y.; Ren, Y.; Häussler, M.; Lam, J. W. Y.; Wong, J. W. Y.; Tang, B. Z. *J. Phys. Chem. B* **2007**, *111*, 2000–2007.

(23) Chen, J.; Xu, B.; Quyang, X.; Tang, B. Z.; Cao, Y. *J. Phys. Chem. A* **2004**, *108*, 7522–7526.

(24) Yuan, C. X.; Tao, X. T.; Wang, L.; Yang, J. X.; Jiang, M. H. *J. Phys. Chem. C* **2009**, *113*, 6809–6814.

(25) Liu, Y.; Tao, X.; Wang, F.; Dang, X.; Zou, D.; Ren, Y.; Jiang, M. *J. Phys. Chem. C* **2008**, *112*, 3975–3981.

(26) Liu, Y.; Tao, X.; Wang, F.; Shi, J.; Sun, J.; Yu, W.; Ren, Y.; Zou, D.; Jiang, M. *J. Phys. Chem. C* **2007**, *111*, 6544–6549.

(27) Zeng, Q.; Li, Z.; Dong, Y.; Di, C.; Qin, A.; Hong, Y.; Ji, L.; Zhu, Z.; Jim, C. K. W.; Yu, G.; Li, Q.; Li, Z.; Liu, Y.; Qin, Y.; Tang, B. Z. *Chem. Commun.* **2007**, 70–72.

(28) Li, Y.; Li, F.; Zhang, H.; Xie, Z.; Xie, W.; Xu, H.; Li, B.; Shen, F.; Ye, L.; Hanif, M.; Ma, D.; Ma, Y. *Chem. Commun.* **2007**, 231–233.

(29) Qian, L.; Tong, B.; Shen, J.; Shi, J.; Zhi, J.; Dong, Y.; Yang, F.; Dong, Y.; Lam, J. W. Y.; Liu, Y.; Tang, B. Z. *J. Phys. Chem. B* **2009**, *113*, 9098–9103.

(30) Yang, Z.; Chi, Z.; Yu, T.; Zhang, X.; Chen, M.; Xu, B.; Liu, S.; Zhang, Y.; Xu, J. *J. Mater. Chem.* **2009**, *19*, 5541–5546.

(31) Yuan, W. Z.; Lu, P.; Chen, S.; Lam, J. W. Y.; Wang, Z.; Liu, Y.; Kwok, H. S.; Ma, Y.; Tang, B. Z. *Adv. Mater.* **2010**, *22*, 1–5.

(32) Xu, B.; Chi, Z.; Yang, Z.; Chen, J.; Deng, S.; Li, H.; Li, X.; Zhang, Y.; Xu, N.; Xu, J. *J. Mater. Chem.* **2010**, *20*, 4135–4141.

(33) Zhao, Z.; Chen, S.; Lam, J. W. Y.; Jim, C. K. W.; Chan, C. Y. K.; Wang, Z.; Lu, P.; Deng, C.; Kwok, H. S.; Ma, Y.; Tang, B. Z. *J. Phys. Chem. C* **2010**, *114*, 7963–7972.

(34) Zhao, Z.; Chen, S.; Lam, J. W. Y.; Lu, P.; Zhong, Y.; Wong, K. S.; Kwok, H. S.; Tang, B. Z. *Chem. Commun.* **2010**, *46*, 2221–2223.

(35) Wang, W.; Lin, T.; Wang, M.; Liu, T. X.; Ren, L.; Chen, D.; Huang, S. *J. Phys. Chem. B* **2010**, *114*, 5983–5988.

(36) Li, Z.; Dong, Y.; Mi, B.; Tang, Y.; Häussler, M.; Tong, H.; Dong, Y.; Lam, J. W. Y.; Ren, Y.; Sung, H. H. Y.; Wong, K. S.; Gao, P.; Williams, I. D.; Kwok, H. S.; Tang, B. Z. *J. Phys. Chem. B* **2005**, *109*, 10061–10066.

(37) Kokado, K.; Chujo, Y. *Macromolecules* **2009**, *42*, 1418–1420.

(38) Qin, A.; Jim, C. K. W.; Tang, Y.; Lam, J. W.Y.; Liu, J.; Mahtab, F.; Gao, P.; Tang, B. Z. *J. Phys. Chem. B* **2008**, *112*, 9281–9288.

(39) Pucci, A.; Rausa, R.; Ciardelli, F. *Macromol. Chem. Phys.* **2008**, *209*, 900–906.

(40) Li, Y.; Vamvounis, G.; Holdcroft, S. *Macromolecules* **2002**, *35*, 6900–6906.

(41) Liu, J.; Lam, J. W. Y.; Tang, B. Z. *J. Inorg. Organomet. Polym.* **2009**, *19*, 249–285.

(42) Lai, C. T.; Hong, J. L. *J. Phys. Chem. C* **2009**, *113*, 18578–18583.

(43) Liu, J.; Zhong, Y.; Lam, J. W. Y.; Lu, P.; Hong, Y.; Yu, Y.; Yue, Y.; Faisal, M.; Sung, H. H. Y.; Williams, I. D.; Wong, K. S.; Tang, B. Z. *Macromolecules* **2010**, *43*, 4921–4936.

(44) Qin, A.; Lam, J. W. Y.; Tang, L.; Jim, C. K. W.; Zhao, H.; Sun, J.; Tang, B. Z. *Macromolecules* **2009**, *42*, 1421–1424.

(45) Lai, J. T.; Hong, J. L. *J. Phys. Chem. B* **2010**, *114*, 10302–10310.

(46) Imai, Y.; Maldar, N. N.; Kakimoto, M. *J. Polym. Sci., Polym. Chem. Ed.* **1984**, *22*, 2189–2196.

(47) Su, F. K.; Hong, J. L.; Lin, L. L. *Synth. Met.* **2004**, *142*, 63–69.

(48) Yang, C. H.; Lin, L. L.; Hong, J. L. *Polym. Int.* **2005**, *54*, 679–685.

(49) Tang, B. Z.; Xu, H. *Macromolecules* **1999**, *32*, 2569–2576.

(50) Sun, Q.; Lam, J. W. Y.; Xu, K.; Xu, H.; Cha, J. A. P.; Wong, P. C. L.; Wen, G.; Zhang, X.; Jing, X.; Wang, F.; Tang, B. Z. *Chem. Mater.* **2000**, *12*, 2617–2624.

(51) Yanari, S. S.; Bovey, F. A.; Lumry, R. *Nature* **1963**, *200*, 242–244.

(52) Hirayama, F. *J. Chem. Phys.* **1965**, *42*, 3163–3171.